Free Radical Research, March 2011; 45(3): 326–335

informa
healthcare

SOD/catalase mimetic platinum nanoparticles inhibit heat-induced apoptosis in human lymphoma U937 and HH cells

YOKO YOSHIHISA[1], QING-LI ZHAO[2], MARIAME ALI HASSAN[2,3], ZHANG-LI WEI[2], MEGUMI FURUICHI[1], YUSEI MIYAMOTO[4], TAKASHI KONDO[2] & TADAMICHI SHIMIZU[1]

[1]*Department of Dermatology, and* [2]*Department of Radiological Sciences, Graduate School of Medicine and Pharmaceutical Sciences, University of Toyama, Toyama, Japan,* [3]*Department of Pharmaceutics and Industrial Pharmacy, Faculty of Pharmacy, Cairo University, Kasr Al-Aini str., Cairo 11562, Egypt, and* [4]*Department of Integrated Biosciences, Graduate School of Frontier Sciences, University of Tokyo, Chiba, Japan*

(Received date: 16 June 2010; In revised form date: 4 October 2010)

Abstract

Platinum nanoparticles (Pt-NPs) are known to possess anti-tumouric activity and the ability to scavenge superoxides and peroxides indicating that they can act as superoxide dismutase (SOD)/catalase mimetics. These potentials seem useful in the protection and/or amelioration of oxidative stress-associated pathologies, but, when they are combined with a therapeutic modality that depends upon the mediation of reactive oxygen species in cell killing induction, the effect of Pt-NPs might be questionable. Here, the effects of polyacrylic acid-capped Pt-NPs (nano-Pts) on hyperthermia (HT)-induced apoptosis and the underlying molecular mechanisms were investigated in human myelomonocytic lymphoma U937 and human cutaneous T-cell lymphoma HH cells. The results showed that the pre-treatment with nano-Pts significantly inhibited HT-induced apoptosis in a dose-dependent manner. Superoxide, but not peroxides, was suppressed to varying extents. All pathways involved in apoptosis execution were also negatively affected. The results reveal that the combination of nano-Pts and HT could result in HT-desensitization.

Keywords: *Platinum nanoparticles, apoptosis, ROS, lymphoma cells*

Abbreviations: *HH, cutaneous T-cell lymphoma (CTCL) cell line; HT, hyperthermia; nano-Pts, platinum nanoparticles; ROS, reactive oxygen species.*

Introduction

The medicinal use of platinum (Pt)-based compounds has been prompted by the discovery of the anti-tumour activity of *cis*-Diamminedichloroplatinum (cis-platin; discovered in 1960 and approved for clinical use in 1978) [1]. Nanomedicine, which aims at improving the efficacies of existing therapeutics, has extended its scope to include Pt in nanoparticles (NPs) in order to promote its innate activity [2]. A recent study showed that platinum nanoparticles (Pt-NPs) were capable of inducing DNA damage and p53-mediated growth arrest [3]. Also, FePt@CoS_2 yolkshell NPs were shown to be more potent in killing HeLa cells compared to *cis*-platin [4].

On the other hand, NPs of some noble metals, including Pt, behave as reducing catalysts owing to their large surface area [5]. In biological systems, this ability imparts a superoxide dismutase (SOD)/catalase mimetic activity to these preparations which could be useful in the prevention and/or the amelioration of a number of oxidative stress-associated pathologies (e.g. inflammatory reactions, cellular

Correspondence: Professor Takashi Kondo, Department of Radiological Sciences, Graduate School of Medicine and Pharmaceutical Sciences, University of Toyama, Sugitani 2630, Toyama, 930-0194, Japan. Tel: +81-76-434-7265. Fax: +81-76-434-5190. Email: kondot@med.u-toyama.ac.jp

ISSN 1071-5762 print/ISSN 1029-2470 online
DOI: 10.3109/10715762.2010.532494

transformation) [6–8]. Moreover, in the real situation cancer is hardly treated with a single modality. Rather, a multimodality therapeutic protocol is usually adopted in which one modality is physical in nature such as hyperthermia or X-irradiation. Physical therapy, as well as some chemotherapeutics, is known to induce an elevation in intracellular reactive oxygen species (ROS) non-selectively in tumour and surrounding normal tissues resulting in post-exposure pathologies. SOD/catalase mimetics have been suggested to be co-administered in such cases to minimize ROS-induced damage to normal tissues and thus alleviate some of the side-effects [1]. Therefore, it is implied from the previous discussion that the presence of Pt-NPs in a biological system can exert a number of effects with positive impact in cancer prevention and treatment. Yet, the knowledge that cell killing is mediated in many cases by an elevation in intracellular ROS raises skepticism about the use of NPs in combination with other modalities. In augmentation, the addition of exogenous free radical scavengers is widely accepted as an ordinary laboratory maneouvre to confirm the role of ROS in the execution of cell killing following different treatments, as manifested by a proportional increase in the final percentage of cell viability. Then it might be that Pt-NPs as potent free radical scavengers and SOD/catalase mimetic [9] result in the reversal of cell killing to an extent detrimental to adjuvant therapy.

To resolve this concern, we have undertaken this study to investigate the effect of Pt-NPs at different concentrations in combination with hyperthermia (44°C, 30 min) on the extent of apoptosis induction since hyperthermia induces apoptosis due to intracellular superoxide formation [10]. Furthermore, we have tried to trace the effect on the micromolecular level through analysing the changes in markers of both the intrinsic and extrinsic pathways. The changes in intracellular ROS formation were also monitored. The Pt-NPs used in this study are capped with polyacrylate (PAA) imparting more stability to their colloidal solution [11]. PAA-capped Pt-NPs (nano-Pts) have been shown to be superior to EUK-8, a well-known SOD/catalase mimetic [12], and their *in vivo* activity has been reported [8].

Materials and methods

Materials

Human myelomonocytic lymphoma U937cell line was obtained from Human Sciences Research Resource Bank (Tokyo, Japan); cutaneous T-cell lymphoma (CTCL) HH cell line was obtained from American Tissue Culture Corporation (Manassas, VA). Hydroethidine (HE), dichlorofluorescein diacetate (DCFH-DA) and dihydrorhodamine 123 (DHR 123) were purchased from Molecular Probes (Eugene, OR). BES-So-AM was from Wako (Tokyo, Japan) and 2-[6-(4-Hydroxy) phenoxy-3H-xanthen-3-on-9-yl] benzoic acid (HPF) was from Daiichi Pure Chemicals Co. (Tokyo, Japan). Anti-Bcl-2 monoclonal antibody (mAb), anti-Bax polyclonal antibody (pAb), anti-Bid pAb and anti-β-actin Ab were purchased from Santa Cruz Biotechnology Inc. (Santa Cruz, CA); Fura-2-AM was from Dojindo Lab (Kumamoto, Japan). Nano-Pts were prepared as described previously [9]. All other reagents were of analytical grade.

Cell culture

Cultured cells were maintained in RPMI 1640 medium (Sigma-Aldrich, Tokyo, Japan) supplemented with 10% heat-inactivated foetal bovine serum (FBS) (SAFC Biosciences, Lenex, KA) at 37°C in humidified air with 5% CO_2. Cell viability before treatment was always over 95%, as evaluated by Trypan blue dye exclusion test. On the day of experiment, cells were collected and suspended in fresh culture medium at a concentration of 1×10^6 cells/ml. The cells were divided into six groups: a control group, group receiving 100 μM of nano-Pts, group treated with hyperthermia (HT; 44°C, 30 min) and another three groups treated with the combination at increasing concentrations of nano-Pts; namely, 10, 50 and 100 μM. The nano-Pts were first added to cells 24 h before HT was applied to designated groups after which analysis was performed at specific time schedules as mentioned for each test.

DNA fragmentation assay

For the detection of apoptosis, the percentage of fragmented DNA was assessed 6 h post-treatment using the method of Sellins and Cohen [13] with minor modifications. In brief, ~ 3×10^6 cells were lysed using 200 μl of lysis buffer (10 mM Tris, 1 mM EDTA, 0.2% Triton X-100, pH 7.5) and centrifuged at 13 000 g for 10 min. Subsequently, DNA from each sample in the supernatant and the pellet was precipitated in 12.5% trichloroacetic acid (TCA) at 4°C overnight and quantified using the diphenylamine reagent after hydrolysis in 5% TCA at 90°C for 20 min. The percentage of fragmented DNA for each sample was calculated as the amount of DNA in the supernatant divided by the total DNA for that sample (supernatant plus pellet).

Assessment of early apoptosis and secondary necrosis

To determine the proportion of early apoptosis and secondary necrosis, cells were collected 6 h post-treatment and stained simultaneously with fluorescein isothiocyanate (FITC)-labelled Annexin V and propidium iodide (PI) according to the instructions of the Annexin V-FITC kit (Immunotech, Marseille,

France) and finally analysed with a flow cytometer (Epics XL, Beckman-Coulter, Miami, FL).

Assessment of intracellular reactive oxygen species (ROS)

Intracellular ROS levels were measured flow cytometrically using a number of fluorescent probes with different affinities to reactive oxygen species. Thus, Hydroethidine (HE) and BES-So-AM were used to confirm the production of superoxide ($O_2^{-\cdot}$) anion and its involvement in apoptosis mediation [14,15], whereas dichlorofluorescein diacetate (DCFH -DA) and dihydrorhodamine 123 (DHR 123) were used to evaluate the involvement of peroxides including hydrogen peroxide (H_2O_2) [16–18]. In addition, 2-[6-(4-Hydroxy) phenoxy-3H-xanthen-3-on -9-yl] benzoic acid (HPF) was also employed to evaluate intracellular hydroxyl ($OH^{\cdot}$) and peroxynitrite ($ONOO^-$) radicals [18]. After 30 min incubation following hyperthermic treatment, cells were stained with 2 μM HE, 50 μM BES-So-AM, 5 μM DCFH-DA, 10 μM HPF or 1 μM DHR 123 and incubated for 15–30 min at 37°C in the dark [19,20]. Finally, cell samples were injected into a flow cytometer for analysis.

Measurement of mitochondrial membrane potential (ΔΨm)

To measure changes in ΔΨm, control cells and cells treated with nano-Pts (100 μM), HT and the combination were collected at 1, 3 and 6 h post-treatment. The cells were then stained with 10 nM tetramethylrhodamine methyl ester (TMRM) (Molecular Probes, Eugene, OR) for 15 min at 37°C in PBS containing 1% FBS. The fluorescence of TMRM was analysed using flow cytometry [21].

Flow cytometric detection of Fas on cell surface

Cells (2×10^5) were washed twice with phosphate buffer saline (PBS), suspended in 20 μl of washing buffer containing 2.5 μg/ml FITC-labelled anti-Fas monoclonal antibody (clone: UB3, MBL, Nagoya, Japan), incubated for 30 min at 37°C and then analysed by flow cytometry [22].

Assessment of intracellular caspase-3 activities

The CaspGlow™ Fluorescein Active Caspase-3 Staining Kit (MBL, Nagoya, Japan) was used to monitor the intracellular caspase-3 activity following the manufacturer's recommendations. Briefly, the cells (1×10^6/ml) were subjected to treatment, 300 μl of each of the samples and control cultures was aliquoted into a microtube after 6 h incubation and 1 μl of FITC-DEVD-FMK was added into each tube followed by incubation for 30 min at 37°C in a 5% CO_2 incubator. The samples were finally analysed by flow cytometry [23].

Determination of intracellular concentration of calcium ions ($[Ca^{2+}]_i$) in single cells

The determination of intracellular free calcium ions ($[Ca^{2+}]_i$) was basically carried out according to the method described previously [24]. Immediately after different treatments, the cells were collected by centrifugation and washed with HEPES-buffered Ringer (HR) solution (118 mM NaCl, 4.7 mM KCl, 2.5 mM $CaCl_2$, 1.13 mM $MgCl_2$, 1 mM Na_2HPO_4, 5.5 mM glucose, 10 mM HEPES- KOH, pH 7.4). The supplemented HR buffer contained 0.2% bovine serum albumin, Eagle's minimal essential amino acids and 2 mM L-glutamine. For dye loading, the cells were suspended at a density of 1×10^5 cells/ml of the supplemented HR and loaded with 5 mM Fura-2-AM for 30 min at 25°C. After washing, digital images of Fura-2 fluorenscence were acquired and analysed using a digital image processor (Argus 50/Ca, Hanamatsu, Japan) coupled to an inverted fluorescence microscope. The ratio of 510 nm emission fluorescence at 340 nm excitation to that at 380 nm excitation, $F(340/380)$, was used as an indicator of $[Ca^{2+}]_i$ in single cells.

Western blot analysis

Cells were collected 6 h post-hyperthermic exposure and washed with cold PBS. The cells were lysed at a density of 1×10^6 cells/50 μl of RIPA buffer (1 M Tris-HCA, 5 M NaCl, 1% Nonidet P-40 (v/v), 1% sodium deoxycholate, 0.05% SDS, 1 mM phenylmethyl sulphonyl fluoride) for 20 min. After brief sonication, the lysates were centrifuged at 12 000 rpm for 10 min at 4°C and the protein content in the supernatant was measured using a Bio-Rad Protein Assay kit (Bio-Rad, Hercles, CA). The protein lysates were denatured at 96°C for 5 min after mixing with 5 μl of sodium dodecyl sulphate (SDS)-loading buffer, applied on an SDS polyacrylamide gel for electrophoresis and transferred to nitrocellulose membrane. Western blot analysis was carried out to detect the expressions of Bcl-2, Bax and Bid using specific antibodies, respectively. Band signals were visualized on X-ray film using chemiluminescence ECL detection reagents (Amersham Biosciences, Buckinghamshire, UK).

Measurement of intracellular Pt content

The cells (1×10^7 cells) treated for 24 h with or without nano-Pts (100 μM) were collected by centrifugation and the pellets were frozen. After thawing, each sample was placed in a glass vessel and

reconstituted in nitric acid and hydrogen peroxide (1:1). The solutions were evaporated to dryness on a hot plate and then the residues were dissolved in dilute aqua regia (4 vol.%). Quantitative analysis of Pt for each solution was performed using inductively coupled plasma mass spectrometry (ICP-MS, Model ELAN DRC II: Perkin Elmer SCIEX. Perkin Elmer Inc., Wellesley, MA).

Statistical analysis

The results are expressed as the mean ± standard deviation (SD) of at least three independent replicates. Statistical significance ($p < 0.05$) was evaluated by one-way ANOVA followed by Bonferroni post-hoc test.

Results

Effect of nano-Pts on HT-induced apoptosis

The exposure of U937 and HH cells to hyperthermic treatment (44°C, 30 min) resulted in a large percentage of apoptotic cell death as manifested by DNA fragmentation which reached up to 56.7 ± 5.9% and 43.4 ± 9.8%, respectively. These percentages had decreased in a concentration-dependent manner upon pre-incubation with nano-Pts at various concentrations (10 ~ 100 μM) for 24 h (Figure 1). The 24 h pre-incubation period was chosen based upon preliminary investigation of the effect of pre-incubation period from 60 min to 24 h in the presence of nano-Pts (100 μM) (data not shown).

In augmentation, the flow cytometric analysis of the membrane changes indicative of different stages of apoptosis progression using annexin V-FITC and PI showed that the percentage of early apoptotic cells decreased from 32.2 ± 2.0% and 24.0 ± 0.6% following HT treatment to 11.0 ± 4.4% and 4.8 ± 2.1% in the presence of 100 μM in U937 cells and HH cells, respectively (Figure 2). On the other hand, the percentage of secondary necrotic cells was unaffected with nano-Pts pre-treatment in both cell lines.

Nano-Pts exert differential inhibition on HT-induced ROS

The inhibitory effects of nano-Pts on HT-induced ROS, namely; $O_2^{-\cdot}$ and peroxides, are plotted in Figure 3. The plots represent the data acquired at 30 min post-hyperthermic treatment based upon time-dependent analyses of ROS at 30 min, 1 and 2 h which showed that ROS peaked at 30 min followed by a time-dependent decrease in both cell lines ($O_2^{-\cdot}$: 89.1 ± 3.3% in U937 and 77.8 ± 3.7% in HH at 30 min; 55.0 ± 1.9% in U937 and 40.0 ± 4.8% in HH at 1 h; 29.4 ± 3.1% in U937 and 34.1 ± 5.4% in HH at 2 h. Peroxides: 51.5 ± 2.5% in U937 and 64.9 ± 3.9% in HH at 30 min; 37.9 ± 2.6% in U937 and 52.5 ± 2.6% in HH at 1 h, 19.0 ± 3.4% in U937 and 21.1 ± 3.6% in HH at 2 h). As shown in Figure 3A, although the HT-induced $O_2^{-\cdot}$ production was completely inhibited in U937 cells in the presence of 100 μM of nano-Pts, only partial inhibition was observed in HH cells under the same experimental conditions. On the other hand, the percentage of cells showing elevated peroxides post-HT treatment did not change after pre-incubation with nano-Pts (Figure 3B). The additional analysis with HPF resulted in very low absolute values indicating that

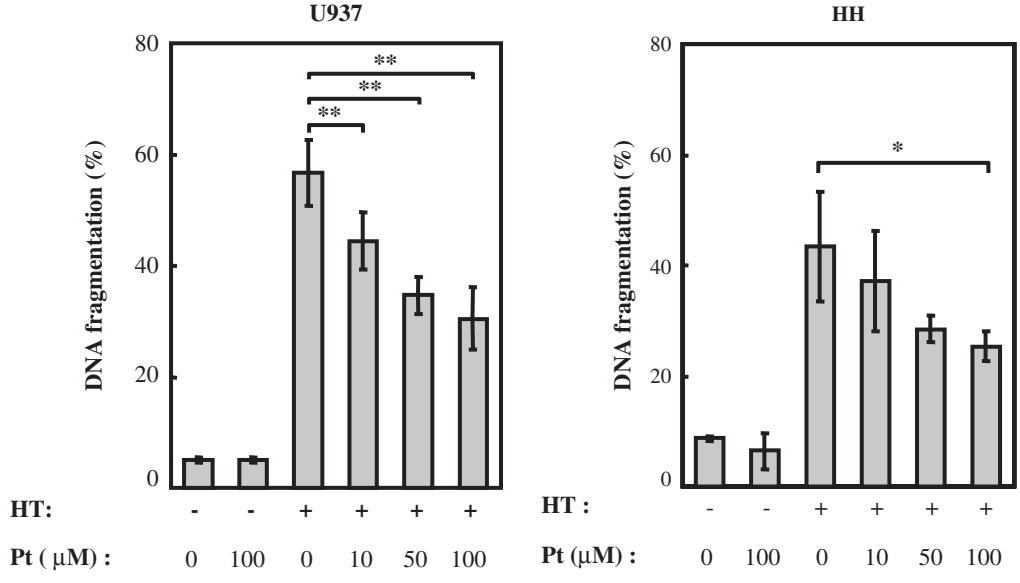

Figure 1. Effects of nano-Pts on HT-induced DNA fragmentation. Cells were treated with HT (44°C, 30 min) with or without a 24-h pre-incubation with nano-Pts at different concentrations. DNA fragmentation assay was carried out at 6 h post-HT exposure. Data are presented as mean ± SD ($n = 5$). $^{*}p < 0.05$, $^{**}p < 0.01$.

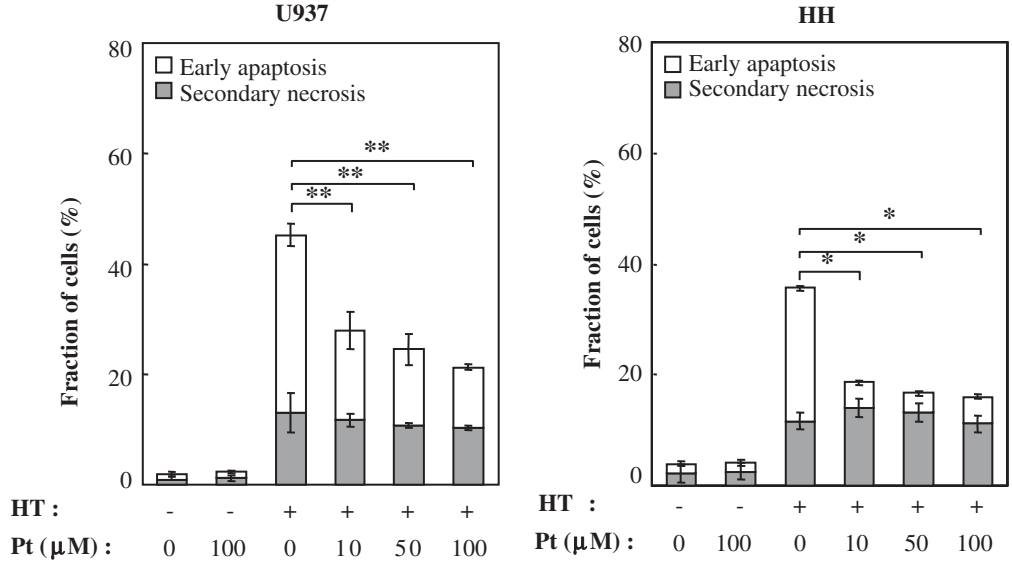

Figure 2. Flow cytometric detection of early apoptosis and secondary necrosis. Cells were treated with HT (44°C, 30 min) with or without a 24-h pre-incubation with nano-Pts at different concentrations. The percentages of early apoptosis (FITC-annexin V+/PI– cells) and secondary necrosis (FITC-annexin V+/PI+ cells) were assessed 6 h after HT using flow cytometry. Data are presented as mean ± SD ($n = 5$). $^{*}p < 0.05$, $^{**}p < 0.01$.

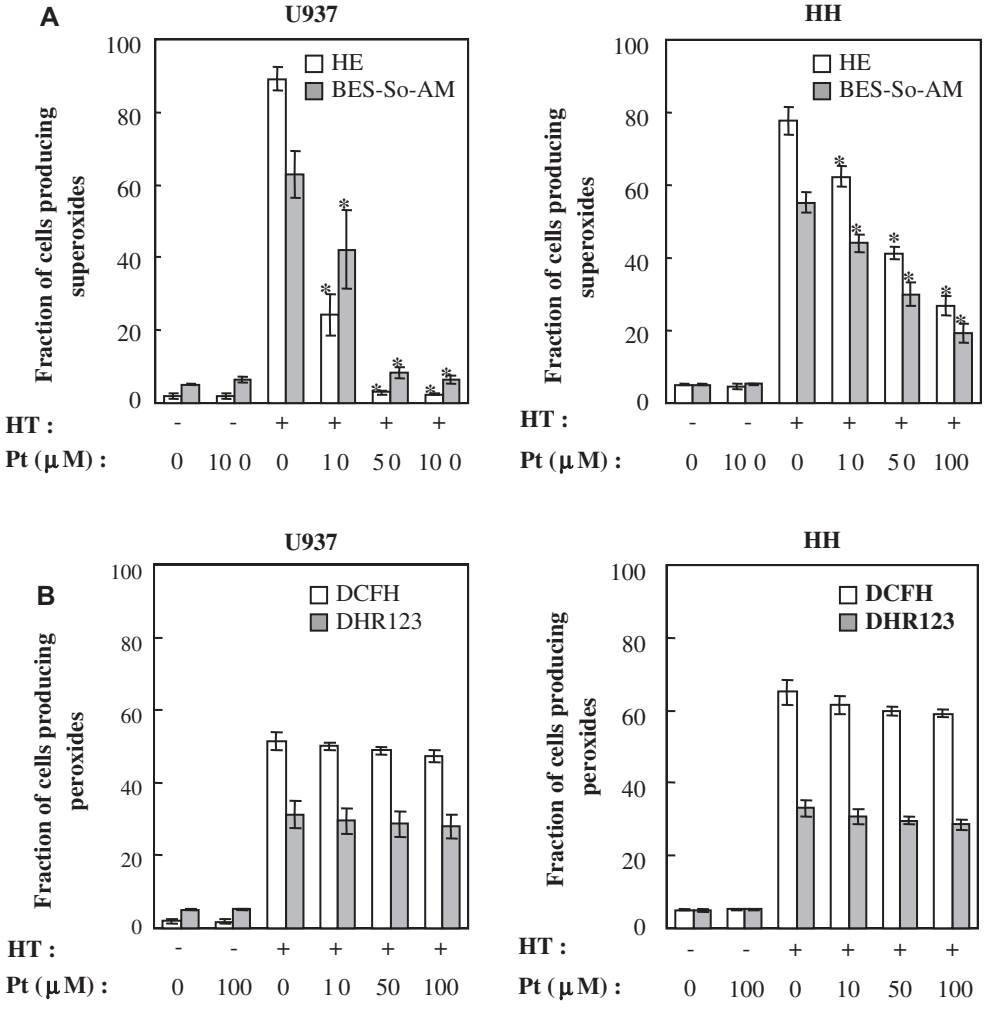

Figure 3. Effects of nano-Pts on HT-induced intracellular ROS production. The percentages of cells with elevated (A) O_2^{-}·, and (B) peroxides analysed at 30 min after HT with flow cytometry. Data are presented as mean ± SD ($n = 5$). $^{*}p < 0.01$.

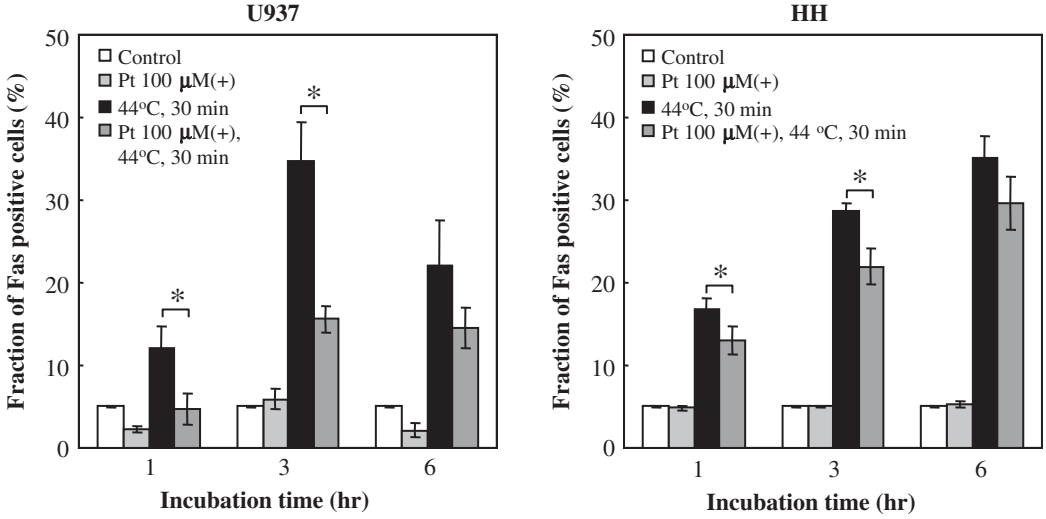

Figure 4. Effects of nano-Pts on HT-induced Fas externalization. The fraction of cells externalizing Fas was analysed by flow cytometry at 1, 3 and 6 h following different treatments. The results are presented as the mean ± SD ($n = 5$). $^{*}p < 0.01$.

the extent of $OH^{\cdot}$ and $ONOO^{-}$ radicals production was very small and unaffected by the presence of nano-Pts (control; 4.8 ± 0.3% in U937 and 5.0 ± 0.3% in HH, HT; 12.3 ± 2.5% in U937 and 12.4 ± 2.0% in HH, HT with nano-Pts (100 μM) 12.0 ± 3.1% in U937 and 12.2 ± 1.7% in HH) while emphasizing the low affinity of HPF to peroxides and $O_2^{-\cdot}$. Conclusively, it is shown the inhibitory effects of nano-Pts on HT-induced ROS are most likely specific to $O_2^{-\cdot}$.

Suppression of Fas receptor externalization by nano-Pts

To examine the effects of nano-Pts on Fas externalization, cells were exposed to HT with or without pre-incubation with 100 μM of nano-Pts. A significant decrease in Fas externalization was observed at 1 h in both cell lines and persisted for 3 h (Figure 4).

Effects of nano-Pts on the mitochondrial pathway

The effect of nano-Pts pre-treatment on the loss of mitochondrial membrane potential (ΔΨm) was investigated. Figure 5 reveals that the pre-incubation with nano-Pts (100 μM) resulted in a conservation of ΔΨm in cells exposed to HT as manifested by the decreased percentage of cells showing loss of ΔΨm at 1, 3 and 6 h in both cell lines.

Analysis of the Ca^{2+}-dependent pathway

It has been reported that the induction of apoptosis in U937 cells is mediated, in part, via a Ca^{2+}-dependent

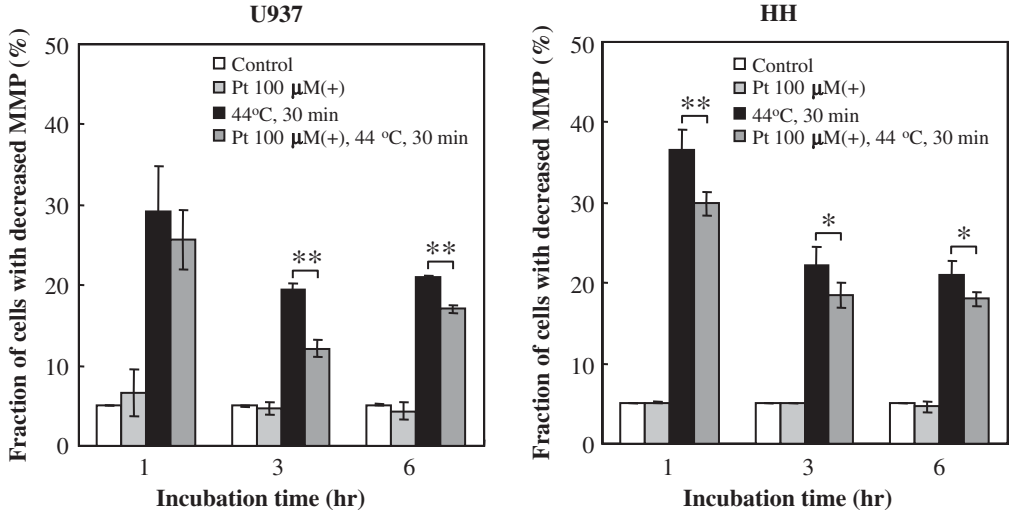

Figure 5. Effects of nano-Pts on HT-induced loss of MMP. Cells were treated with HT (44°C, 30 min) with or without a 24-h pre-incubation with 100 μM nano-Pts. At 1, 3 and 6 h following different treatments, the percentage of MMP loss was analysed by flow cytometry using TMRM staining. Data are presented as mean ± SD ($n = 5$). $^{*}p < 0.05$, $^{**}p < 0.01$.

pathway, specifically through the Ca^{2+}/Mg^{2+}-dependent DNase and calpain activation [25,26]. Thus, it was speculated that the role of nano-Pts in the reduction of HT-induced apoptosis might involve changes in the intracellular $[Ca^{2+}]_i$. Therefore, the $[Ca^{2+}]_i$ in a single cell was measured by a digital image analysing technique using Fura-2 in U937 and in HH cells as well after HT treatment and/or nano-Pts. The pseudocolour

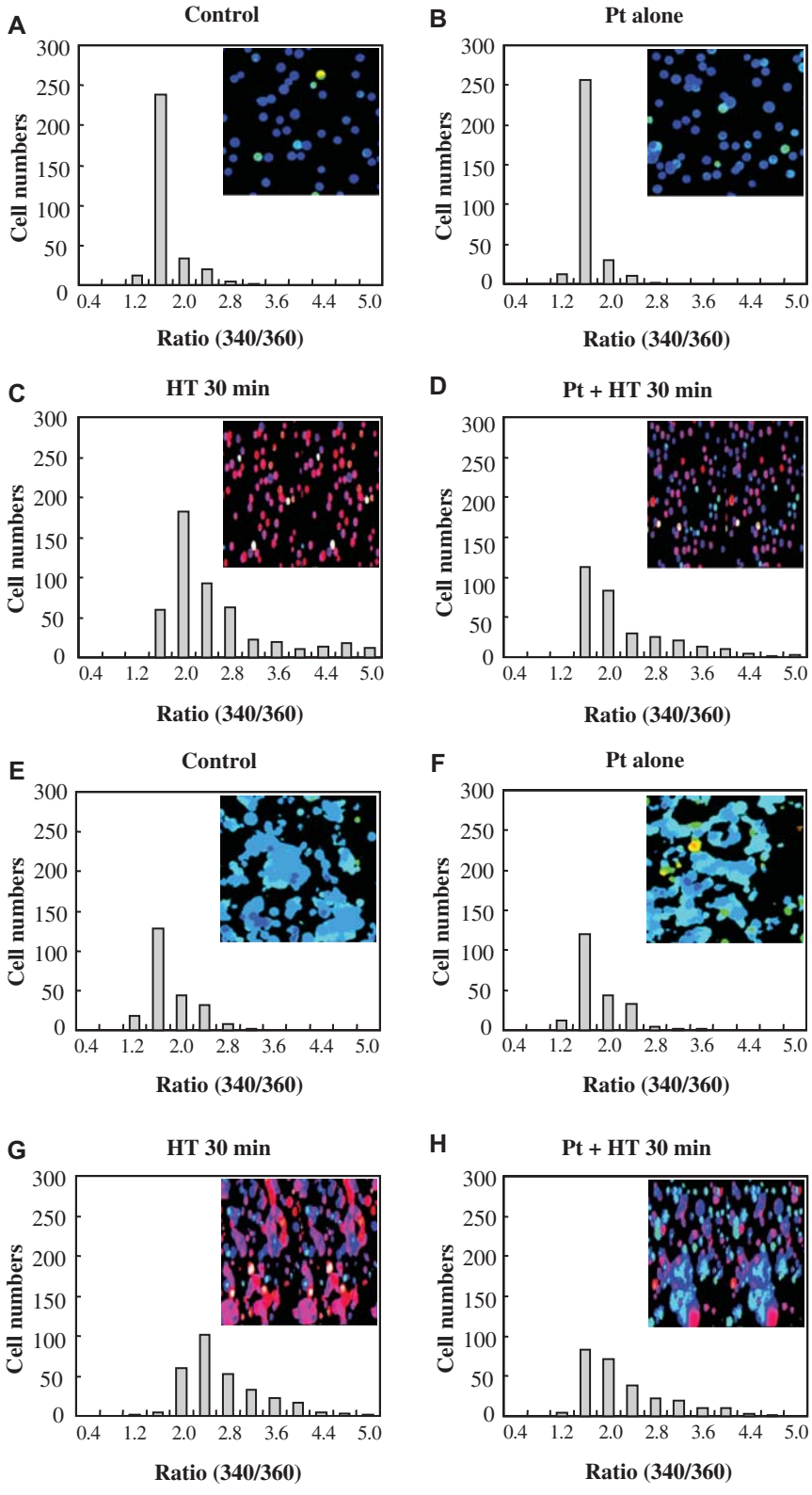

Figure 6. Effects of nano-Pts on HT-induced $[Ca^{2+}]_i$ concentration. Cells were stained with Fura-2-AM immediately after different treatments. (A–D) HT-induced $[Ca^{2+}]_i$ concentration in U937 cells. (E–H) HT-induced $[Ca^{2+}]_i$ concentration in HH cells . (A) and (E) Untreated controls; (B) and (F) nano-Pts alone; (C) and (G) HT; (D) and (H) nano-Pts (100 μM) + HT. The data shown are representatives of five independent experiments.

images of $[Ca^{2+}]_i$ in individual cells shown in Figure 6 (insets) show an increase in $[Ca^{2+}]_i$ following HT, whereas a decrease was observed when a combination of HT and nano-Pts was used. These effects were observed in both cell lines, indicating that nano-Pts could reverse HT-induced apoptosis.

Measurement of intracellular Pt content

When the intracellular content of Pt in samples was measured by ICP-MS, the values were 5.6 ± 0.1 ng for treated cells and < 0.05 ng for untreated control cells. Thus, significant intracellular incorporation of Pt was observed.

Expression of apoptosis-related proteins

The western blotting revealed that the expression of Bid was decreased post-HT treatment in U937 and HH cells, whereas the pre-incubation with nano-Pts resulted in an increase in its expression. However, no apparent change in the expression of Bax and Bcl-2 was found in both cell lines (Figure 7A). Moreover, the nano-Pts pre-treatment resulted in a significant decrease in caspase-3 activity compared to HT alone in both cells (Figure 7B).

Discussion

As the results showed, the concern raised upon using nano-Pts in combination with HT turned out to be valid in concept. Nano-Pts were able to suppress the HT-induced apoptosis in both cell lines in a concentration-dependent manner. Moreover, the data unveiled a number of findings that need sophisticated efforts to explain in the future. For example, it has been reported that similar PAA-protected Pt-NPs were able to accumulate cells in the S-phase 48 h post-treatment, accompanied by an increase in the sub-G1 cells indicative of apoptotic cell death. Based on this, it would have been expected that HT should increase the exerted lethal effect owing to the knowledge that S-phase cells are more heat-sensitive [27], especially that G2/M cells did not

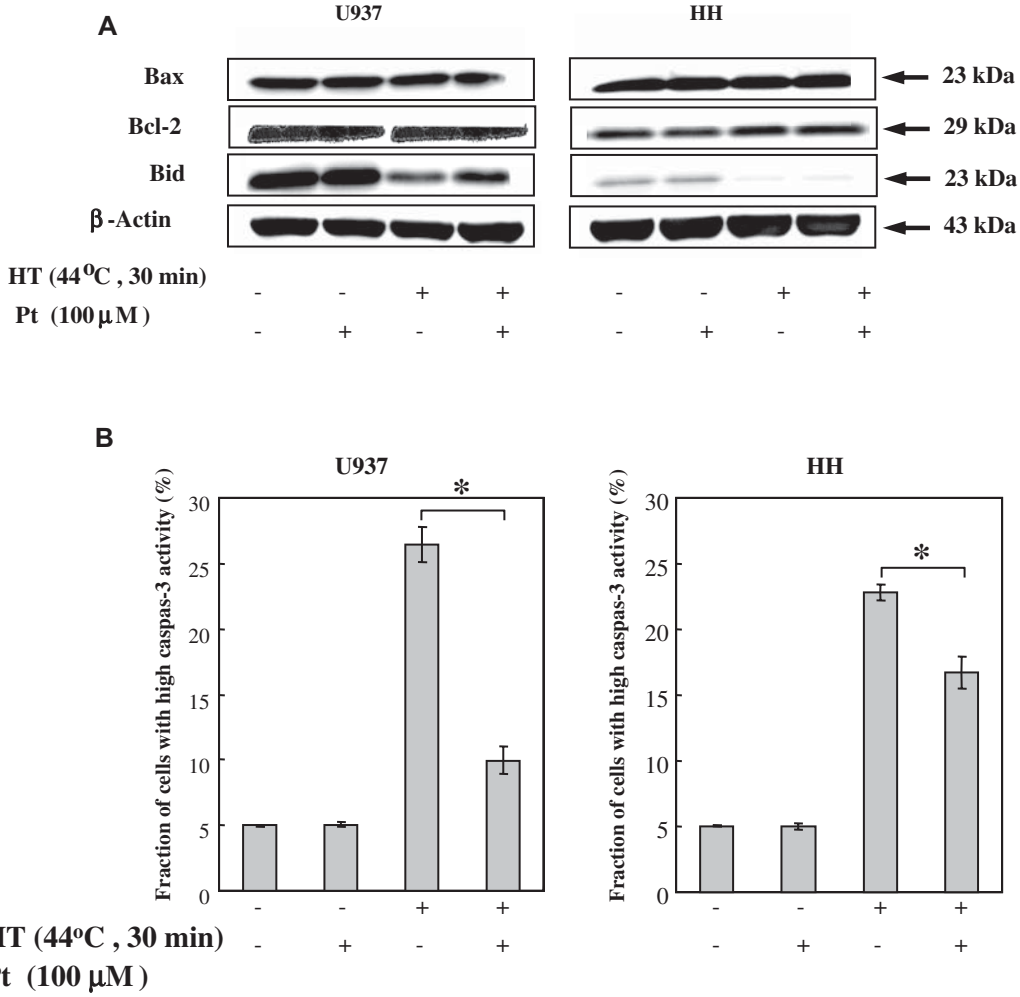

Figure 7. Western blotting of apoptosis-related proteins. Cells were pre-incubated with or without nano-Pts (100 μM) for 24 h before HT treatment and then allowed to incubate for a further 6 h. (A) Western blot analysis of Bax, Bcl-2 and Bid proteins (30 μg protein in each group). (B) CaspGlowTM Fluorescein Active Caspase-3 Staining Kit used to evaluate caspase-3 activity. The data shown are representatives of three independent experiments. Data are presented as mean ± SD ($n = 5$). $^*p < 0.01$.

show any change in presence of nano-Pts. In our case, there was a reversal of HT lethal effect in the presence of nano-Pts at relative concentrations. Although this could be explained by the differences in the time point analyses performed in the two studies, it might be more comprehensive that the low percentage of the S-phase arrest shown (ca. 6%) was not enough to counteract the potent scavenging activity of nano-Pts.

We reported that nano-Pts effectively protects against UV-induced inflammation by decreasing ROS production and inhibiting apoptosis in keratinocytes [7]. Another finding, which is concerned with the antioxidant potential of these preparations previously reported in a number of studies, is that they were only able to decrease the $O_2^{\cdot -}$ elevation and not the peroxides, regardless of the cell line. Added to this discrepancy is the reported durability of nano-Pts in scavenging ROS. Not only does this phenomenon raise questions about the exact mechanism of action exerted by nano-Pts in combination with HT, but also about the differential significance of both ROS species for the execution of apoptosis. Concerning the later aspect, it has been shown that HT-induced apoptosis in HL-60 cells was partially inhibited by catalase and not by SOD [28]. On the other hand, $O_2^{\cdot -}$ was reported to be involved with HT-induced apoptosis in U937 cells [29]. Thereupon, the selective changes in ROS might reflect that the $O_2^{\cdot -}$ suppression, as well as the suppression of both extrinsic and intrinsic pathways and the Ca^{2+}-dependent pathway, was a consequence of the pre-treatment with nano-Pts prior to HT rather than a causative of the reversal observed. In line with this postulation is the trial to encapsulate Pt-NPs in apoferritin in order to reduce the stress on cellular membrane caused by the adsorbed NPs [30]. Also a recent discovery reported on the reconstruction of phospholipid membranes where the phase transition temperature can deviate by 'tens of degrees' as a consequence of the interaction with NPs depending on their charge [31]. Thereupon, a role on the cell membrane level might exist whereas an intracellular role on the protein level cannot yet be excluded in the desensitization of cells to HT.

According to the previous discussion, though not explicit, our findings might not relate to the SOD/catalase activity of nano-Pts. If it were the antioxidant activity that justifies for the partial reversal of HT-induced apoptosis, one might think that the same effect should be observed with X-irradiation. In contrast, Porcel et al. [2] have found that DNA damage was more prone in the presence of Pt. Furthermore, the group showed that DNA samples loaded with PAA–capped Pt-NPs exhibited increased damage with a sensitizing factor for double strand breaks (DSBs) higher than that for single strand breaks (SSBs) indicative of more complex breaks in the presence of NPs compared to Pt atoms. Despite lacking the complete biological environment required for accurate judgement, these results basically highlight the flaw in generalizing multimodality cancer therapy protocols. Furthermore, they add to the significance of our study being devoted to HT and nano-Pts combination.

In conclusion, we have shown, for the first time, that the pre-treatment with nano-Pts prior to HT exposure was able to reverse the HT-induced apoptosis through a suppression of all the involved micromolecular pathways. Moreover, there was selective suppression in ROS elevation in both cell lines indicative of other modes of action exerted by nano-Pts that are apart from their SOD/catalase activity.

Declaration of interest

This research was supported by a Grant-in-Aid for Scientific Research (C) (No. 20591337) and (B) (No. 22390229) from the Japan Society for the Promotion of Science. The authors report no conflicts of interest. The authors alone are responsible for the content and writing of the paper.

References

[1] Bhattacharya R, Mukherjee P. Biological properties of 'naked' metal nanoparticles. Adv Drug Deliv Rev 2008; 60:1289–1306.

[2] Porcel E, Liehn S, Remita H, Usami N, Kobayashi K, Furusawa Y, Le Sech C, Lacombe S. Platinum nanoparticles: a promising material for future cancer therapy? Nanotechnology 2010;21:85103.

[3] Asharani PV, Xinyi N, Hande MP, Valiyaveettil S. DNA damage and p53-mediated growth arrest in human cells treated with platinum nanoparticles. Nanomedicine (Lond) 2010; 5:51–64.

[4] Gao J, Liang G, Zhang B, Kuang Y, Zhang X, Xu B. FePt@ CoS(2) yolk-shell nanocrystals as a potent agent to kill HeLa cells. J Am Chem Soc 2007;129:1428–1433.

[5] Toshima N, Yonezawa T. Bimetallic nanoparticlesnovel materials for chemical and physical applications. New J Chem 1998;22:1179–1201.

[6] Valko M, Leibfritz D, Moncola J, Cronin MTD, Mazura M, Telser J. Free radicals and antioxidants in normal physiological functions and human disease. Int J Biochem Cell Biol 2007;39:44–84.

[7] Yoshihisa Y, Honda A, Zhao QL, Makino T, Abe R, Matsui K, Shimizu H, Miyamoto Y, Kondo T, Shimizu T. Protective effects of platinum nanoparticles against UV-light-induced epidermal inflammation. Exp Dermatol 2010. (in press)

[8] Onizawa S, Aoshiba K, Kajita M, Miyamoto Y, Nagai A. Platinum nanoparticle antioxidants inhibit pulmonary inflammation in mice exposed to cigarette smoke. Pulm Pharmacol Ther 2009;22:340–349.

[9] Kajita M, Hikosaka K, Iitsuka M, Kanayama A, Toshima N, Miyamoto Y. Platinum nanoparticle is a useful scavenger of superoxide anion and hydrogen peroxide. Free Radic Res 2007;41:615–626.

[10] Hirano H, Tabuchi Y, Kondo T, Zhao QL, Ogawa R, Cui ZG, Feril LB, Jr, Kanayama S. Analysis of gene expression in apoptosis of human lymphoma U937 cells induced by heat

shock and the effects of alpha-phenyl N-tert-butylnitrone (PBN) and its derivatives. Apoptosis 2005;10:331–340.
[11] Roucoux A, Schulz J, Patin H. Reduced transition metal colloids: a novel family of reusable catalysts? Chem Rev 2002;102:3757–3778.
[12] Kim J, Takahashi M, Shimizu T, Shirasawa T, Kajita K, Kanayama A, Miyamoto Y. Effects of a potent antioxidant, platinum nanoparticle, on the lifespan of Caenorhabditis elegans. Mech Ageing Dev 2008;129:322–331.
[13] Sellins KS, Cohen JJ. Gene induction by gamma-irradiation leads to DNA fragmentation in lymphocytes. J Immunol 1987;139:3199–3206.
[14] Gorman A, McGowan A, Cotter TG. Role of peroxide and superoxide anion during tumour cell apoptosis. FEBS Lett 1997;404:27–33.
[15] Maeda H, Yamamoto K, Kohno I, Hafsi L, Itoh N, Nakagawa S, Kanagawa N, Suzuki K, Uno T. Design of a practical fluorescent probe for superoxide based on protection-deprotection chemistry of fluoresceins with benzenesulfonyl protecting groups. Chemistry 2007;13:1946–1954.
[16] Qin Y, Lu M, Gong X. Dihydrorhodamine 123 is superior to 2,7-dichlorodihydrofluorescein diacetate and dihydrorhodamine 6G in detecting intracellular hydrogen peroxide in tumor cells. Cell Biol Int 2008;32:224–228.
[17] Huang HL, Wu SL, Liao HF, Jiang CI, Huang RL, Chen YY, Yang YC, Chen YJ. Induction of apoptosis by three marine algae through generation of reactive oxygen species in human leukemic cell lines. J Agric Food Chem 2005;53:1776–1781.
[18] Crow JP. Dichlorodihydrofluorescein and dihydrorhodamine 123 are sensitive indicators of peroxynitrite *in vitro*: implications for intracellular measurement of reactive nitrogen and oxygen species. Nitric Oxide 1997;1:145–157.
[19] Setsukinai K, Urano Y, Kakinuma K, Majima HJ, Nagano T. Development of novel fluorescence probes that can reliably detect reactive oxygen species and distinguish specific species. J Biol Chem 2003;278:3170–3175.
[20] Capella MA, Capella LS, Valente RC, Gefé M, Lopes AG. Vanadate-induced cell death is dissociated from H_2O_2 generation. Cell Biol Toxicol 2007;23:413–420.

This paper was first published online on Early Online on 4 November 2010.

[21] Zhao QL, Fujiwara Y, Kondo T. Mechanism of cell death induction by nitroxide and hyperthermia. Free Radic Biol Med 2006;40:1131–1143.
[22] Cui ZG, Kondo T, Matsumoto H. Enhancement of apoptosis by nitric oxide released from alpha-phenyl-tert-butyl nitrone under hyperthermic conditions. J Cell Physiol 2006;206:468–476.
[23] Datta R, Kojima H, Yoshida K, Kufe D. Caspase-3-mediated cleavage of protein kinase C h in induction of apoptosis. J Biol Chem 1997;272:20317–20320.
[24] Kondo T, Kano E, Habara Y, Kanno T. Enhancement of cell killing and increase in cytosolic calcium concentration by combined treatment with hyperthermia and TMB-8 in mouse mammary carcinoma FM3A cells. Cell Calc 1993;14:621–629.
[25] Kimura C, Zhao QL, Kondo T, Amatsu M, Fujiwara Y. Mechanism of UV-induced apoptosis in human leukemia cells: roles of Ca^{2+}/Mg^{2+}-dependent endonuclease, caspase-3, and stress-activated protein kinases. Exp Cell Res 1998;239:411–422.
[26] Arai Y, Kondo T, Tanabe K, Zhao QL, Li FJ, Ogawa R, Li M, Kasuya M. Enhancement of hyperthermia-induced apoptosis by local anesthetics on human histiocytic lymphoma U937 cells. J Biol Chem 2002;277:18986–18993.
[27] Bhuyan BK. Kinetics of cell kill by hyperthermia. Cancer Res 1979;39:2277–2284.
[28] Katschinski DM, Boos K, Schindler SG, Fandrey J. Pivotal role of reactive oxygen species as intracellular mediators of hyperthermia-induced apoptosis. J Biol Chem 2000;275:21094–21098.
[29] Cui ZG, Kondo T, Feril LB, Jr, Waki K, Inanami O, Kuwabara M. Effects of antioxidants on X-ray- or hyperthermia-induced apoptosis in human lymphoma U937 cells. Apoptosis 2004;9:757–763.
[30] Zhang L, Laug L, Münchgesang W, Pippel E, Gösele U, Brandsch M, Knez M. Reducing stress on cells with apoferritin-encapsulated platinum nanoparticles. Nano Lett 2010;10:219–223.
[31] Wang B, Zhang L, Bae SC, Granick S. Nanoparticle-induced surface reconstruction of phospholipid membranes. Proc Natl Acad Sci USA 2008;105:18171–18175.